Finite Element Study of the Subsidence in Longwall Coal Mines

K. Rajagopal
Professor

P.L.S. Ramakanth
Former M.S. Scholar

Department of Civil Engineering
Indian Institute of Technology Madras
Chennai - 600 036, India
Phone No. 044-445 8298/8320; Fax: 044 235 0509
e-mail: gopal@civil.iitm.ernet.in

ABSTRACT

The mining induced subsidence leads to damage to structures and other facilities at the ground surface. Numerical methods have proved to be very effective tools for the prediction of the ground response due to tunneling activities. This paper discusses the finite element analysis of subsidence due to longwall coal mining which is very common in this country. The first part of this paper discusses the verification of the numerical procedures by comparing the predicted responses with the reported surface subsidence data at two coal mines. The second part of the paper discusses the parametric study to investigate the effect of different factors such as the width of tunnel, space between the different tunnels, depth of mining, in situ earth pressures etc. that influence the surface subsidence. The exact modelling of the vertical and horizontal joints was found to be necessary to obtain accurate predictions. The ratio between the width of the panel and the depth of overburden (w/h) was found to be a critical factor in the mine subsidence. The subsidence was found to be smaller when w/h ratio is less than about 1.2 and increased drastically when w/h ratio approached 1.3 to 1.40. The subsidence was found to be smaller in case of soils with very high lateral earth pressures (i.e. with high K_o). Some important conclusions have been made at the end of the paper based on the results from these numerical simulation studies.

Key Words: Subsidence, mining, longwall mining, finite element analysis, in situ earth pressures, rock joints.

1. INTRODUCTION

The mining for coal, ore and other mineral resources is common around the world. In terms of the procedures followed, the mining can be categorised as

open cast mining, longwall mining and room and pillar mining. The open cast mining is used in case of mineral deposits occurring at shallow depths like at Neyveli Lignite mines. The longwall and room and pillar mining methods are used to extract minerals from large depths by digging tunnels. The longwall mining is the most preferred method of mining in soft rocks like coal. It is suitable in cases with ore body dip of less than 20^o. In this method, the coal is extracted and stope face advanced by mechanically shearing the coal seam by translation of cutting device parallel to the coal seam. This process simultaneously cuts the coal deposit and loads the broken coal into armoured conveyors, by which it is transported to roadway lying parallel to the direction of the face advance. All face operations take place within a working domain protected by a set of hydraulic roof supports. The preferred condition for this method of mining is that the immediate roof rock for coal seam consists of relatively weak shales, siltstones to promote caving. The seam floor rock must have sufficient bearing capacity to support the loads applied by roof support system.

The ground subsidence due to mining activities is an inevitable problem in the coal industry. An underground excavation creates cavities by removing the natural support from the overlying strata. Hence the successive layers of rock undergo bending due to gravity and collapse over the cavity, until finally the movement reaches the surface, resulting in subsidence (Singh, 1978). Due to inadequate understanding of the strata in the past and the consequent ignorance of resulting subsidence, a lot of damage has occurred to surface structures. To prevent damage to surface structures, it is required to restrict the subsidence within the allowable limits. With increase in urbanization and growing concern for the environment, subsidence can no longer be ignored.

Empirical methods commonly used for prediction of subsidence often do not provide an accurate assessment of subsidence profiles, particularly when complex geometries and soil/rock layers are involved. Such complicated geometries and soil profiles can be easily accounted for in the finite element based numerical methods. A number of researchers have used this technique to successfully estimate the mining induced subsidence, e.g. Choi and Dahl (1981), Kohli (1984), Siriwardane (1985) etc. The subsidence at Singareni coal mines was predicted successfully by Naik and Rao (1999) using distinct element code.

The influence of various factors that affect the surface subsidence due to longwall mining is studied in this paper through finite element based numerical simulations.

2. FINITE ELEMENT PROCEDURE

All finite element analyses in this investigation were performed using a computer program GEOFEM originally developed by the principal author at the Royal Military College of Canada and significantly updated at IIT Madras, Rajagopal (1998).

The incremental finite element equilibrium equations considered are of the type shown in Equation 1 in which the load vector is expressed as the difference between the external load vector and the internal reaction force vector computed from the element stresses of the previous iteration.

$$[K]\{\Delta u_i\} = \{P\}_{exti} - \Sigma[B]^T \{\sigma_{i-1}\} \quad (1)$$

in which the 1st term on the RHS is the applied force vector and the 2nd term on the RHS is the internal nodal force vector (reaction force vector). This analysis scheme allows for carrying forward any error in the out-of-balance forces to the next iteration (or next load step) thus satisfying the global equilibrium at all the load steps. This scheme also allows for ease in excavation of elements as the contribution of elements that are just excavated are included in the 2nd term on RHS while their contribution is not included in the force term at the current step in 1st term on RHS. Hence, the difference between the two terms gives the traction force necessary to make the excavated surface a traction free surface. The finite element solutions in this investigation were iterated until the out-of-balance force norm is less than 0.5%.

The in situ stresses with at rest earth pressure coefficient (K_o) plays an important role in the strength and stiffness behaviour of soil. The initial stress state in the soil before any external loads are applied will be $\sigma_z = \gamma z$ where $\gamma$is the unit weight of soil and z is the depth below the free surface of soil. Then the lateral earth pressures $\sigma_x = \sigma_y$ will be equal to $K_o\ \sigma_z$ in which K_o is the coefficient of lateral earth pressure at rest and zero shear stresses for level ground. This state of stress can easily be created in the finite element analyses by performing an initial dummy analysis with a modified Poisson's ratio (μ) whose value can be derived from the fundamental Hooke's equations by setting the two lateral strain terms to zero as,

$$\mu = \frac{K_o}{1 + K_o} \quad (2)$$

In order to simulate the zero lateral strain, the nodes on the vertical boundaries on the two sides should have zero lateral displacements. The desired in situ stresses were obtained in the 1st phase of all analyses by assigning the above Poisson's ratio value to all the materials in the mesh. All materials were also assigned the same Young's modulus values so that undue shear stresses are not generated in the continuum elements during the self-weight analysis. After these stresses are generated, the displacements and the strains within all elements in the mesh were set to zero and further analyses were performed using the actual Poisson's ratio of the soil.

The excavation of coal layers was simulated by physically removing the elements corresponding to the coal layers and applying boundary forces along the free surface created due to the excavation such that the boundary becomes a traction free surface. As the elements are removed from the mesh, their contribution in the overall stiffness of the system was also not considered.

The various steps in the analysis are as follows:

- First step is the self-weight analysis with the modified Poisson's ratio (μ') that leads to the desired in situ earth pressure coefficient (K_o),
- Set all resulting displacements and strains at the end of the above step to zero,
- Gradually remove the elements corresponding to the coal layers and apply boundary forces in the opposite direction to make the excavated surface a traction free surface as illustrated in Fig. 1. This step required the analysis to be performed over a large number of load steps with several iterations per load step. The convergence of the solution was verified by monitoring the norm of the out-of-balance forces. The out-of-balance forces are computed as the difference between the applied loads and the internal nodal reaction as shown on the right hand side term in Eq. 1.

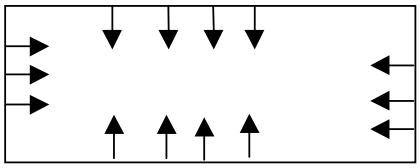

Fig. 1 - Schematic of boundary forces on the tunnel surface to create traction free surfaces

The tunnel roof was allowed to deform freely under the action of the out-of-balance forces. In some cases, the tunnel roof had deflected vertically much more than the thickness of the coal seam excavated because of large overburden depths. In such cases, a displacement control analysis was followed in which all the nodes on the tunnel roof are pulled down by a distance equal to the thickness of the coal seam. The schematic for applying these boundary displacements is shown in Fig. 2. The nodes at the two corners of the tunnel roof were left free to deform on their own while the intermediate nodes are applied the displacement constraints as shown. The nodes adjacent to the two corner nodes were given a displacement equal to half the seam thickness in order to have smooth transition at the edges.

3. ANALYSIS OF FIELD CASES

In the initial part of this investigation, the finite element procedures employed in the analysis were verified by back-predicting the ground subsidence profiles reported at Singareni coal mines (Naik and Rao 1999) and Applachian coal

mines in USA (Su 1992). Both the coal mines employed longwall method of mining to extract the coal.

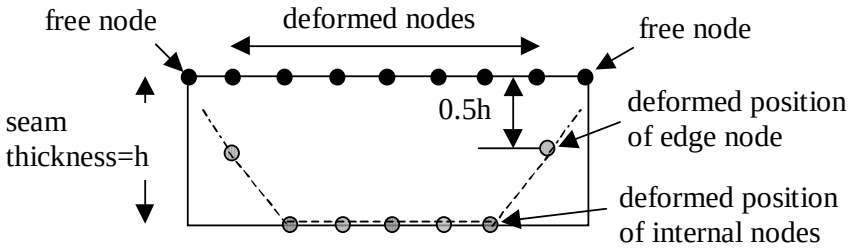

Fig. 2 - Application of displacements to nodes on tunnel roof

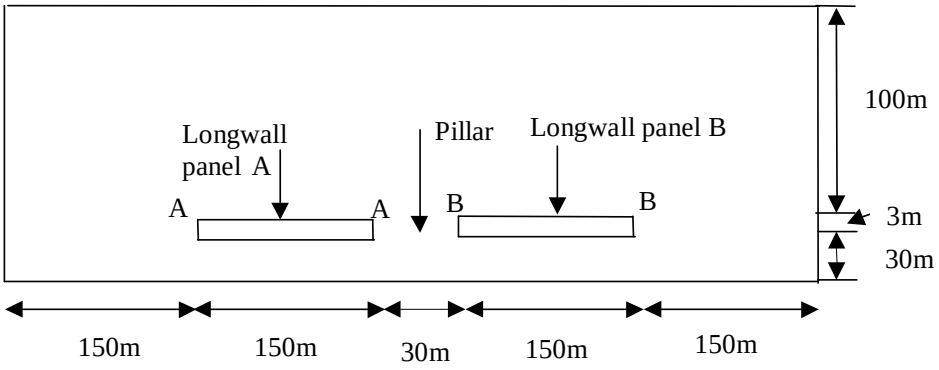

Fig. 3 - Schematic longwall panels at Singareni coal mines

3.1 Subsidence at Singareni Coal Mines

The surface subsidence at Singareni coal mines is very acute with surface subsidences exceeding 2 m. The coal at the site is extracted from a depth of 100 m from twin panels (A and B) having widths of 150 m and separated by a 30 m wide pillar. The thickness of the coal extracted at the site is 3 m, Fig. 3. The coal was first extracted from Panel-A and then Panel-B. The soil is predominantly homogeneous with horizontal bedding planes at 10 m vertical intervals to a depth of 75 m below the ground surface and at 2 m vertical intervals beyond that depth. The vertical joints at the site were observed to be at 20 m horizontal intervals. The properties of the different soil layers and the bedding planes at the site as reported by Naik and Rao (1999) are given in Table 1. The shear and normal stiffness values reported in the table were determined through large-scale field tests conducted on exposed joints at the site, Naik and Rao (1999).

The soil and coal materials were modelled using elastic-perfectly plastic models based on Mohr-Coulomb yield criteria with material properties given in Table 1. When the analyses were performed with even small dilation angles ($\psi \approx 10°$), significant ground heaving was predicted by the finite element model

which was not observed at the site. Hence, all the analyses were performed by setting the dilation angle to zero.

Table 1 - Properties of soil layers at Singareni coal mines

Properties	Coal	Non-coal	Bedding planes/joints
Young's modulus, GPa.	2.58	13	-
Poisson's ratio	0.3	0.28	-
Unit weight kN/m^3	15.9	22.0	-
Cohesion MPa.	2	3.7	0
Friction angle	20°	43°	30°
Normal stiffness, MPa/m.	-	-	417
Shear stiffness, MPa/m.	-	-	167

The stiffness matrix of the joint elements was defined in terms of shear and normal stiffness values. The initial values of these two parameters are given in Table 1. The shear stresses within these interface elements were limited to those given by the Mohr-Coulomb yield limit. When the shear stress exceeds the shear strength as defined by Mohr-Coulomb yield limit, the shear stress was reset to the yield limit and the shear stiffness was reduced to $1/1000^{th}$ of the initial value. The stiffness of joint elements in the normal direction was set to the value shown in Table 1 as long as the element is in compression. When the normal stress in the interface element becomes tensile, its normal stress was set to zero and the stiffness in the normal direction was set to $1/1000^{th}$ of the initial stiffness value.

A finite element mesh was developed consisting of 8-node quadrilaterals and 6-node joint elements to simulate this field case. The mesh consisted of totally 7,417 nodal points, 1484 continuum elements to represent the soil and 1,252 joint elements to represent the horizontal and vertical joints. A typical mesh configuration used to simulate the vertical and horizontal joints is shown in Fig. 4.

The in situ stresses at the site were reported to be with an earth pressure coefficient (K_o) of 0.6. This state of in situ stresses were generated by applying the body forces due to the weight of elements with a Poisson's ratio value of $\mu=K_o/(1+K_o)=0.375$ in the initial analysis. The resulting strains in the elements and nodal displacements were set to zero at the end of this stage and the analysis was re-started after setting the Poisson's ratio values to the actual values.

In the second stage of analysis, the excavation of the coal of 3 m thickness in Panel-A was taken up. This excavation was simulated by removing the elements within that region from the assembly and applying the nodal equivalent forces of the nodes on that surface in the reverse direction to make that boundary a traction free surface. The analysis in this step was performed in small steps by removing coal in 0.5 m increments with up to 1000 iterations

at each load step to achieve convergence of solution. This analysis had predicted a vertical settlement of the tunnel roof of approximately 17 m because of the presence of large number of horizontal and vertical joints and also because of significant overburden above the tunnel roof. As the thickness of the coal extracted is only 3 m, this deformation of much more than 3 m is not possible. This magnitude of the predicted ground subsidence of about 6 m is also much higher than the measured settlement of about 2 m.

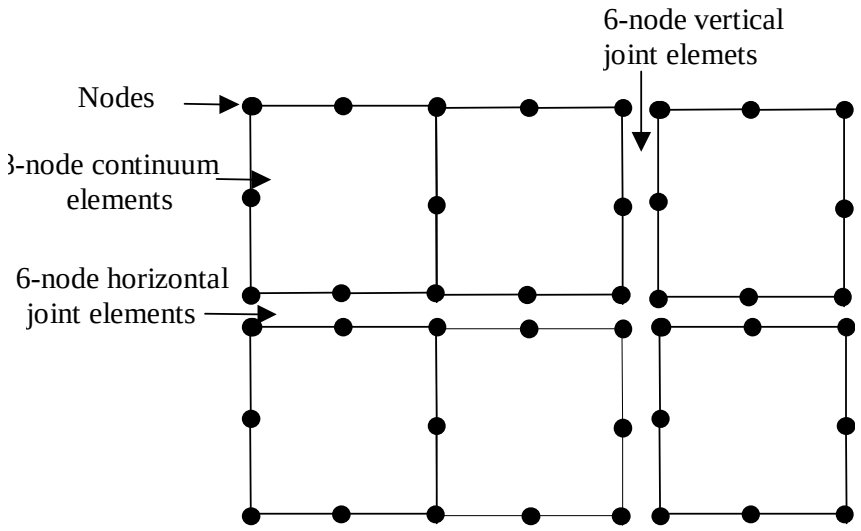

Fig. 4 - Finite element details to represent horizontal and vertical joints

Hence, the above method of analysis has to be changed by restraining the maximum subsidence of the tunnel roof to 3 m. This was simulated approximately by prescribing vertical downward displacement of 3 m to all the nodes on the tunnel roof, except the corner nodes as schematically illustrated in Figure 2. The corner node is left as a free node as it is connected to non-excavated material. The node next to the corner node was prescribed only 1.5 m displacement in order to provide for a smooth transition from the edges to the middle part of the tunnel roof. The analysis was stopped when the nodes just touch the bottom face of the excavation and not continued further. The excavation was done sequentially one panel after the other, i.e. the coal in Panel A was first removed and then the coal in Panel B is removed. The analysis consisted of totally 2001 load steps and up to 75 iterations per load step. In the 1^{st} load step, the self weight of the soil was applied and in the steps 2^{nd} to 1001, the soil in panel-A was removed and vertical downward displacements were applied to the nodes on the tunnel roof. The excavation of soil in Panel-B and the displacement application to the nodes on the tunnel roof were performed from load steps 1002 to 2001. The total analysis took approximately 24 hours of CPU time on a dedicated 266 Hz Pentium computer. The comparative CPU time taken by the discrete element method for the same problem was reported to be about 7 days, Naik and Rao (1999). In order to avoid problems due to power breakdowns, the analysis was split

into a number of steps and the program was repeatedly stopped and re-started. When the program is re-started, it reads all the data pertaining to the previous step as the initial data for further analysis.

The deformed mesh just above the longwall Panel-A after the analysis was completed is shown in Fig. 5. It clearly shows that the mechanism of deformation of the overburden is like the bending of a deep continuous beam. It could be expected that severe tensile stresses be generated within some portion of the overburden. It could be observed in this figure that significant relative deformations took place between different parts of the soil. This was possible due to the inclusion of joint elements in both horizontal and vertical directions.

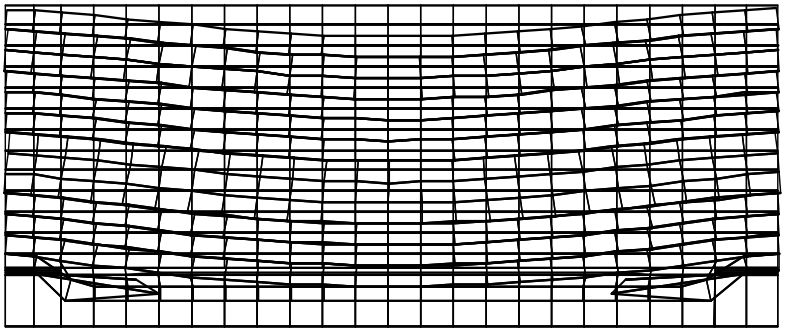

Fig. 5 - Close-up view of deformed mesh above Panel A

The comparison between the predicted and the measured ground surface subsidence is shown in Fig. 6. The maximum measured subsidence above the panel-A is 2.2 m while the predicted value is 1.49 m. Both the predicted and the measured maximum subsidence above panel-B are around 1.30 m. The ground surface above panel-A undergoes further subsidence while the coal from panel-B is extracted. Hence, the subsidence is higher above Panel-A than on panel-B. The finite element analysis has also predicted the same tendency of higher subsidence in panel-A than in panel-B. The maximum measured subsidence above the pillar portion is about 0.15 m while the predicted value is much lower at around 0.05 m. The measured and predicted settlements above panel-B are in very good agreement while there is a large discrepancy over panel A. The refinement of the mesh did not improve the results any further. The reason for the discrepancy between the measured and predicted responses could be attributed to the difference between the actual material properties in the field and those used in the analysis. The width of the predicted and measured settlement bowls at the ground surface over both the panels are quite comparable indicating that the finite element model is able to successfully replicate the lateral spread of the subsidence zone.

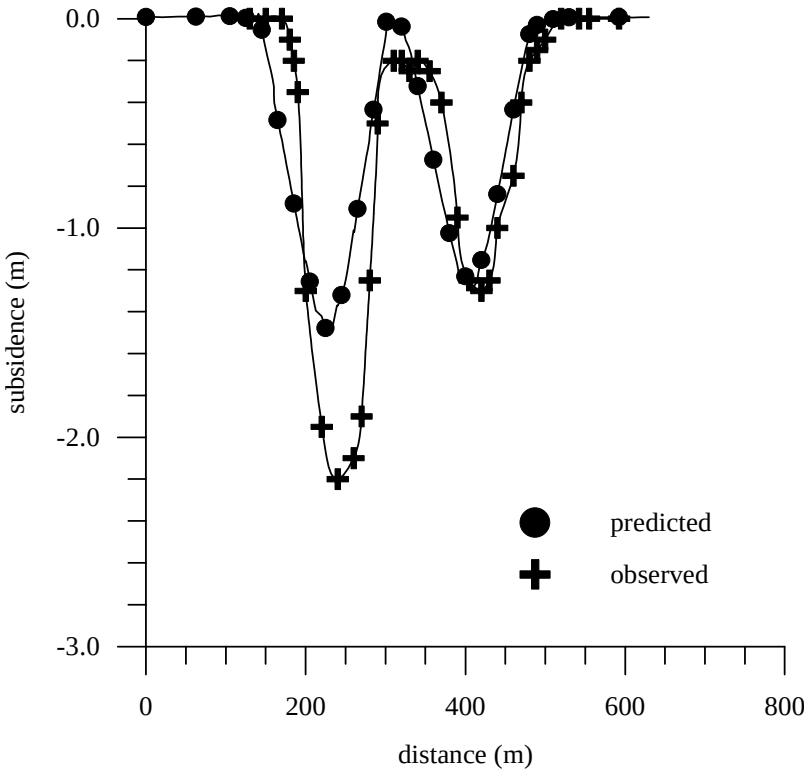

Fig. 6 - Comparison between the predicted and measured surface settlements at Singareni coal mines

3.2 Subsidence at Appalachian Coal Mines

The second field case studied was the case of subsidence at Appalachian coal mines in USA, Su (1992). The coal at this site was mined from a depth of 216.4 m (710 ft). The width of each panel was 182.9 m (600 ft) and the width of the barrier pillar was 77.72 m (255 ft). The thickness of extraction was 1.83 m (6 ft). By considering symmetry, a mesh of length 612.3 m (2009 ft) and a height of 255.72 m (839 ft) was used to simulate this field problem. The soil at the site consisted of eleven distinct layers with varying properties as shown in Table 2.

The finite element mesh for this analysis consists of 8149 nodal points, 1802 eight-node quadrilateral and 1272 six-node joint elements. The analysis consists totally of 2001 load steps as explained earlier. Each load step was iterated a maximum of 75 times to achieve convergence of solution. Sequential excavations were performed in 2^{nd} and 1002^{nd} load steps as explained in the earlier section. After the elements were excavated, the nodes on the tunnel roof were given a vertical downward displacement of 1.829 m to simulate the collapse of tunnel roof to the tunnel floor due to excavation. The entire analysis took approximately 26 hours of CPU time on a Pentium computer with a speed of 266 MHz. This CPU time was split over several

small stages of analysis to overcome the problems due to power failures as described earlier.

Typical excellent comparison between the predicted and the measured field subsidence at Appalachian coal mines is shown in Fig. 7.

Table 2 - Properties of overburden rocks at Appalachian mines

Soil layers below ground surface	Young's modulus (GPa)	Poisson's ratio	Cohesion (MPa)	Friction angle (degree)
Sandstone	22.14	0.22	13.82	42
SW sandstone	14.76	0.22	18.27	33
RS Limestone	17.71	0.22	16.24	38
FP Limestone	29.52	0.18	20.67	40
Shale with sandstone	11.81	0.25	11.42	26
BW Limestone	22.14	0.22	9.39	38
Limey Shale	14.76	0.25	13.82	35
Interbedded shale	11.81	0.25	11.95	35
Surface material	1.181	0.35	1.476	25
Coal	2.95	0.35	6.327	35
Claystone	8.85	0.30	5.314	30

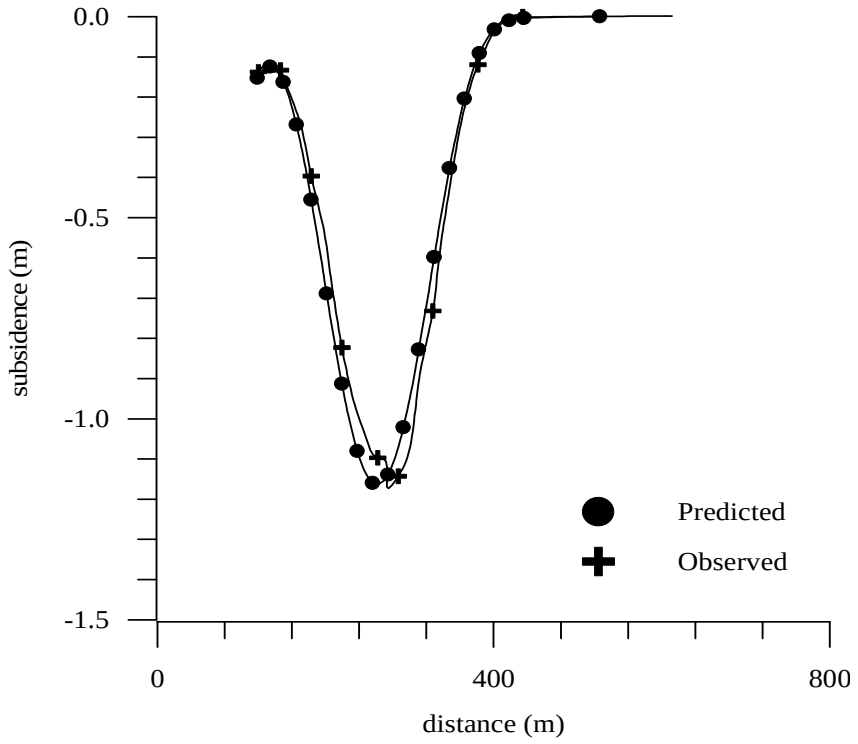

Fig. 7 - Predicted and measured ground subsidence at Applachian coal mines

The good comparison obtained between the finite element predicted and the field observed subsidence shows that the finite element procedures employed are able to simulate the mining induced subsidence reasonably accurate.

4. PARAMETRIC STUDIES

The ground subsidence due to coal extraction depends on a number of factors such as the depth from which the coal is extracted, the width of the panel with respect to the depth of overburden, the pillar width, in situ stress state etc. In order to understand the effect of these factors, a series of parametric studies have been performed as described in the following sub-sections. In all these studies, the soil was assumed as homogeneous without any joints. It is difficult to generalise the joint spacing and their properties as they are site specific. The finite element scheme described earlier has been used in these parametric studies also.

The material properties used in these parametric studies are: Young's modulus of 100,000 kPa, Poisson's ratio of 0.30, cohesive strength of 500 kPa, friction angle (ϕ) of 35°, and unit weight of 20 kN/m^3. A few analyses were also performed with a friction angle of 45°. The earth pressure coefficient was assumed as 0.43. All analyses were performed using plane strain idealisation.

Two different cases were considered in these analyses, one with twin panels and the other with a single panel. The case with a single panel is equivalent to the twin panel case with very large pillar width. The schematic diagrams for these two cases are given in Figs. 8 and 9.

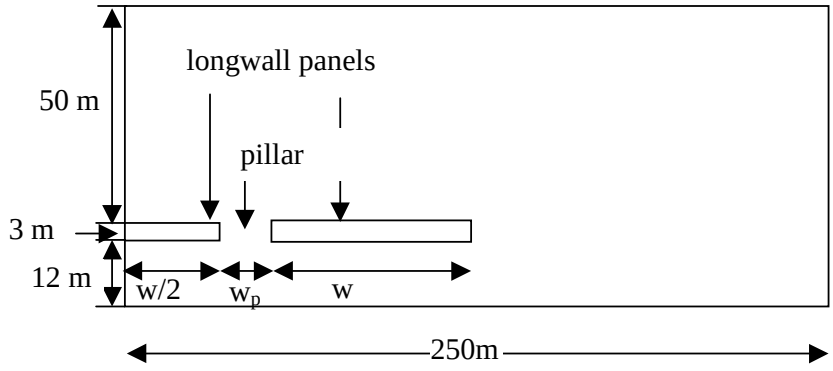

Fig. 8 - Schematic of the finite element mesh with twin longwall panels for parametric studies

4.1 Influence of Geometry of Panels

Two different geometric cases were considered in this series. In the first case, the depth of overburden (h) was kept constant at 50 m and the analyses were performed for five different widths of the twin panels (w) 40, 60, 70, 80 and 100 m. The pillar width in all these analyses was kept constant at 20 m. In the second case, the panel width (w) was kept constant at 40 m (w/h=0.8) and the

analyses were performed with different pillar widths (w_p) of 5, 10, 20 and 30 m. In all the analyses, the w/h ratio was varied from 0.80 to 2.0.

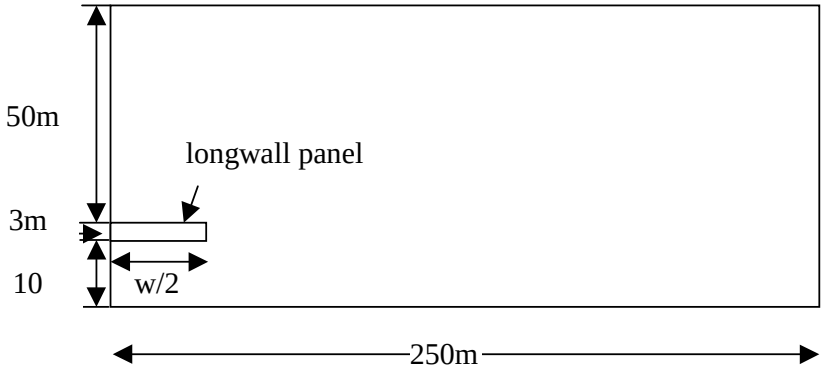

Fig. 9 - Schematic of the finite element mesh with single longwall panel

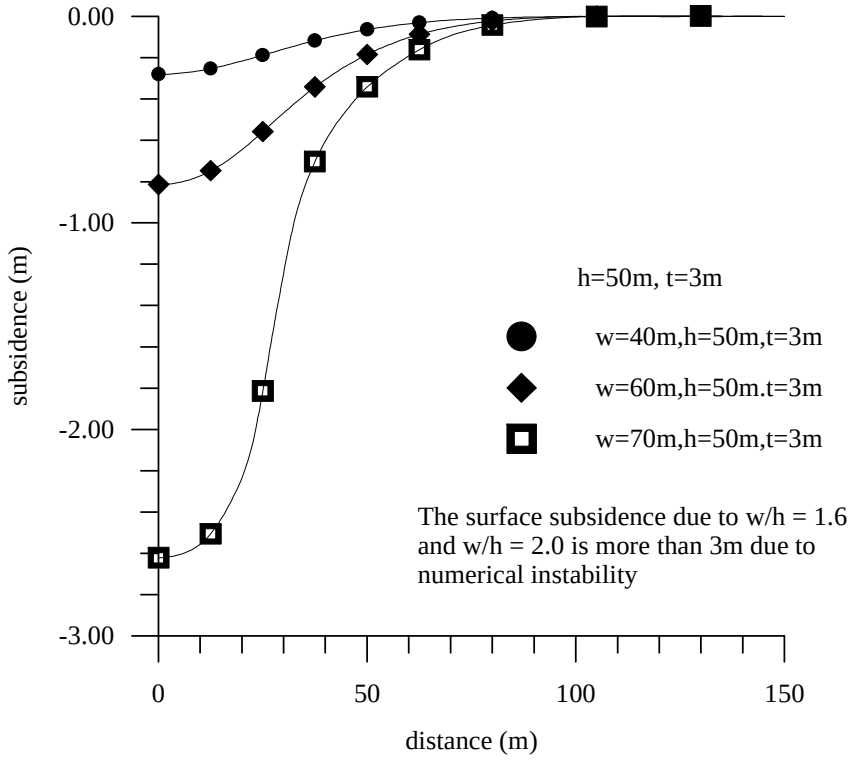

Fig. 10 - Surface subsidence profiles with different w/h ratios

The surface subsidence with different panel widths (single panel) is shown in Fig. 10. It is clear from this figure that as the w/h ratio goes beyond 1.2, the surface subsidence increases rapidly. An examination of the major principal stress contours in the soil shows that as the w/h ratio approaches 1.4, the zone of tensile stresses (and the zone in which the soil has failed) has extended to the ground surface, Figs. 11 and 12. From these figures, it could be observed that in the case of w/h ratio of 0.8, the tensile stresses are present only in a small region above the tunnel roof while in the case of w/h=1.4, the tensile

stresses have reached the ground surface. Clear rupture planes develop once the tensile stresses reach the ground surface. Similar result was observed with other geometries also. It can also be observed that the width of the surface subsidence bowl increases with the w/h ratio.

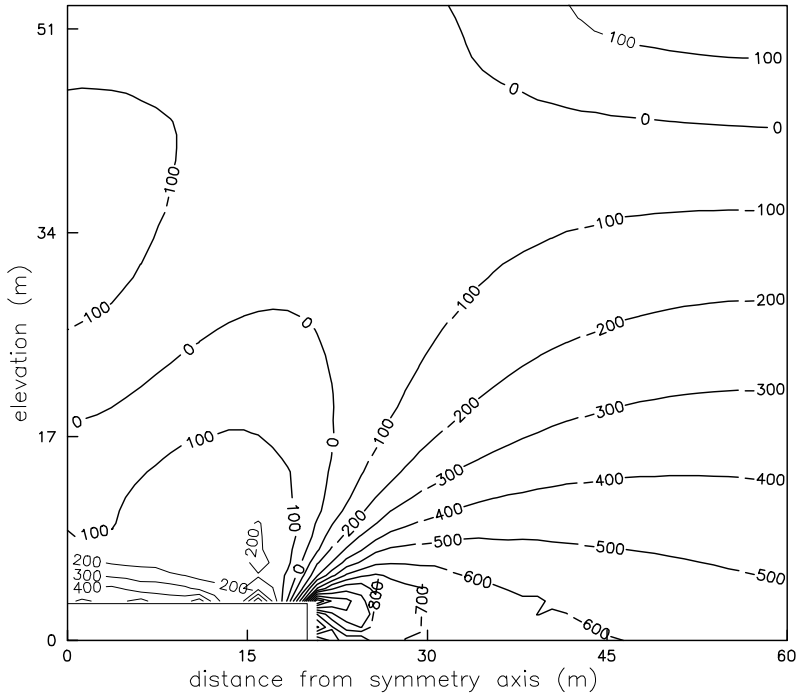

Fig. 11- Major principal stress contours with w/h = 0.80

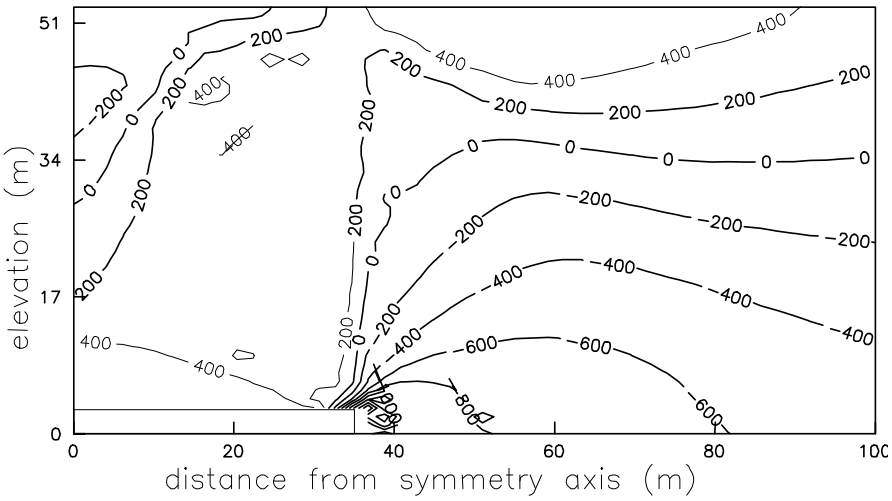

Fig. 12 - Major principal stress contours with w/h = 1.4

The comparison of results from the analyses with twin panels and different pillar widths is shown Fig. 13. It can be observed that at small pillar widths, the twin panels have behaved as a single panel while at higher pillar widths, they have behaved as two independent panels (indicated with two surface

subsidence bowls). When the pillar width was increased to 40 m, no substantial change in behaviour was obtained. As the pillar width increases, the economy of mining operations may be jeopardized because much of coal remains unexplored in the ground. Hence, an optimum pillar width that gives the least surface subsidence needs to be selected. For this particular case, it can be said that the optimum pillar width to obtain least surface subsidence is 30 m.

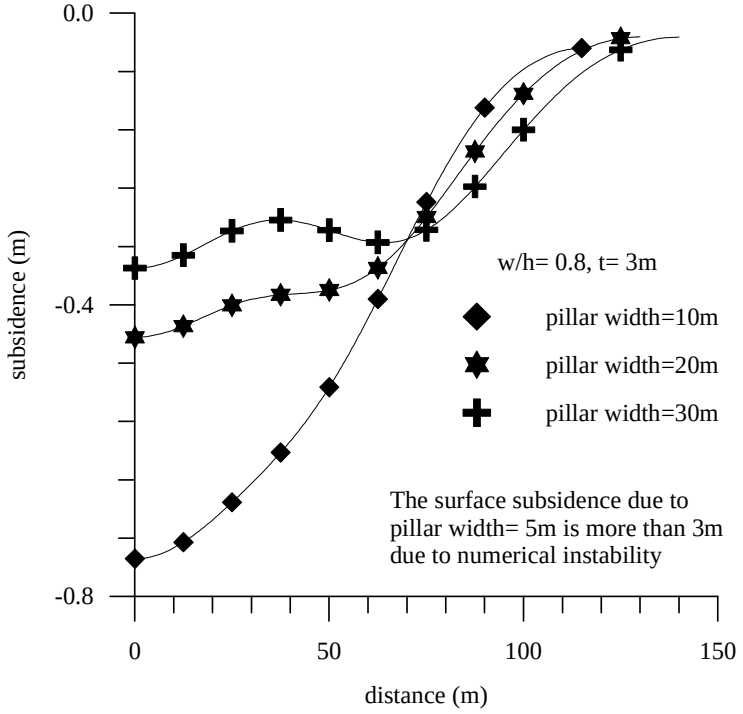

Fig. 13 - Surface subsidence profiles with different pillar widths (w/h = 0.80)

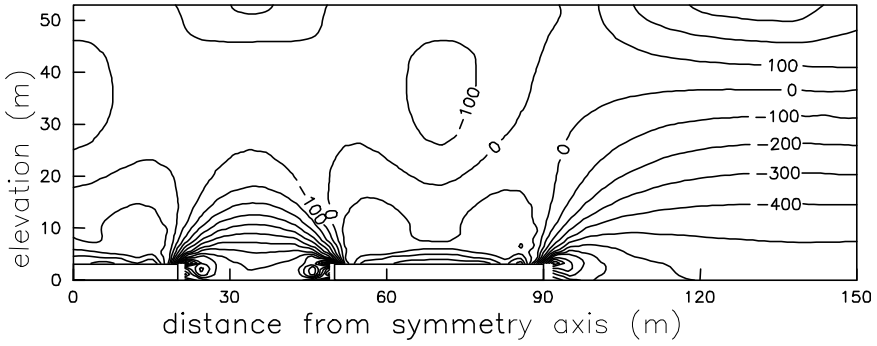

Fig. 14 - major principal stress contours with pillar width of 30m

The major principal stress contours with pillar widths of 30 m and 5 m are shown in Figs. 14 and 15. While the tensile stresses have occurred only around the tunnel opening with pillar width of 30 m, they have spread up to the ground level when the pillar width was decreased to 5 m.

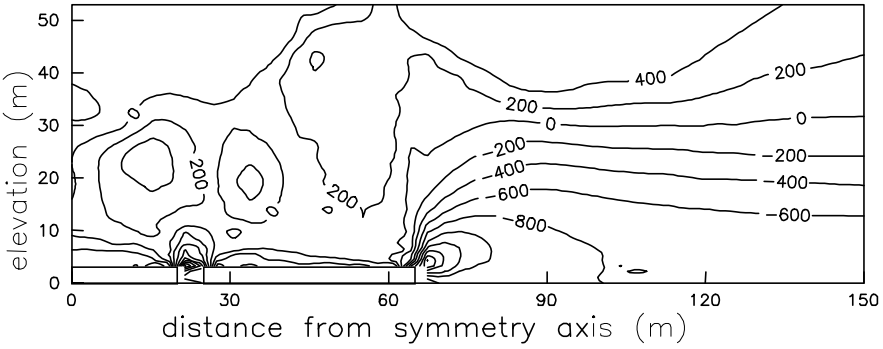

Fig. 15 - Major principal stress contours with pillar width of 5m

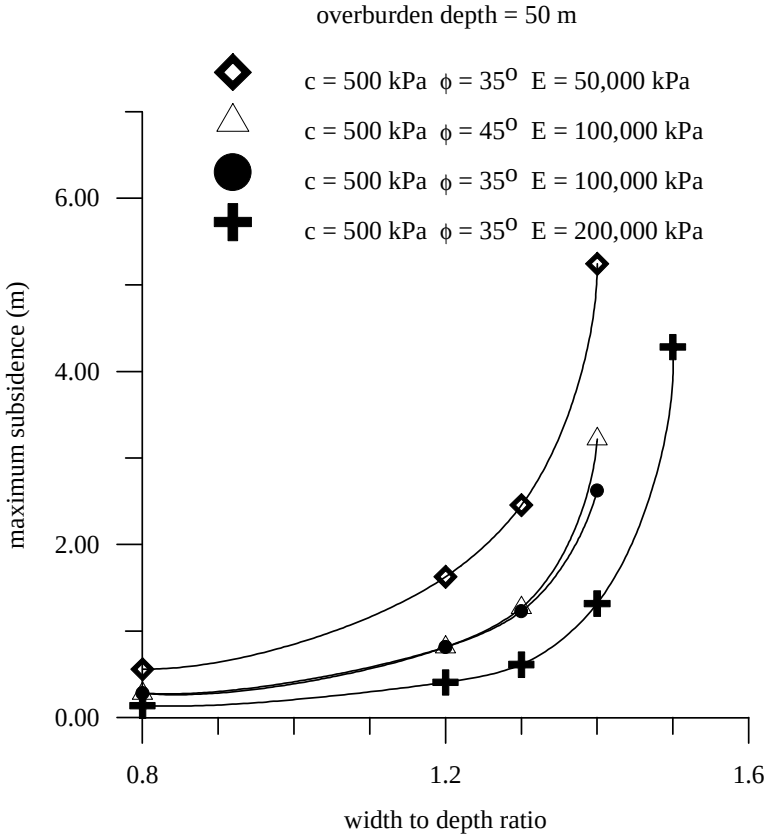

Fig. 16 - Maximum surface subsidences with different panel widths

The maximum subsidence values obtained with different w/h ratios in the case of single panel are shown in Fig. 16. In all the cases, the w/h ratio of about 1.2 is critical at or beyond which the surface subsidence is very large. Hence, this value of w/h may be defined as the *critical value*.

A few analyses were also performed with 100m overburden depth. The trends observed with this depth also were found to be very much similar to those

observed with 50 m overburden depth, i.e. critical w/h ratio, spread of tensile stresses over the soil etc.

4.2 Influence of Friction Angle

The influence of the friction angle on the surface subsidence was studied by performing additional analyses with a friction angle of 45°. All other properties used were as listed earlier. The predicted maximum surface subsidence values with different panel widths are compared in Fig. 16. As could be observed from the figure, the higher friction angle did not influence the surface subsidence for both sub-critical and critical panel widths. The reason for this could be explained as follows. The tensile strength of cohesive soils can be written as $c.\cot\phi$. Hence, the tensile capacity of the soil with cohesive strength of 500 kPa and friction angles of 35° and 45° are 714 and 500 kPa respectively. Hence, the soil with lower friction angle would have higher tensile capacity while having lower frictional capacity. The effects of increase in tensile capacity and the lower frictional capacity may have cancelled each other to a large extent for the particular shear strength properties considered in this investigation. Hence, there was not much difference in the predicted settlements with friction angles of 35° and 45°.

4.3 Influence of In Situ Earth Pressures

All the analyses in this series were performed with single panel. These analyses were performed with different in situ earth pressure coefficients (K_o) of 0.43, 1.0 and 2.0 for different w/h values. The maximum surface subsidence observed with different K_o values are shown in Fig. 17. It is interesting to note that the K_o has no influence on the surface subsidence at w/h ratio of 0.80 while at higher w/h values, the surface subsidence is lower with higher K_o values. The higher initial K_o value in the soil will keep the soil under compressive stresses even after the tunnel is excavated leading to improved performance. This effect can be clearly seen in major principal stress contours for the case of w/h=1.60 and K_o=2.0, Fig. 18. Although the w/h value is much higher than the critical value, the stresses over much of the soil have remained compressive because of high K_o value. The effect of higher K_o at critical values of w/h ratios is similar to the beneficial effect of pre-stressing on the performance of concrete beams.

4.4 Influence of Other Factors

The analysis with different coal seam thickness values has shown that the surface subsidence is not linearly proportional to the thickness of the coal seam thickness. Similarly, the subsidence is not exactly proportional to the Young's modulus.

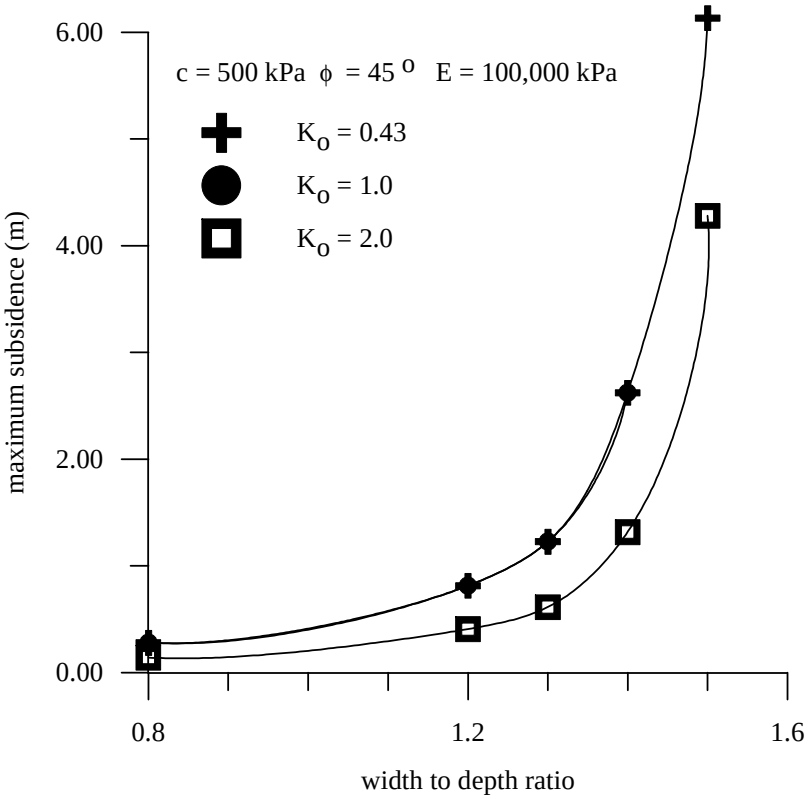

Fig. 17 - Maximum surface subsidence with different K_o and w/h values

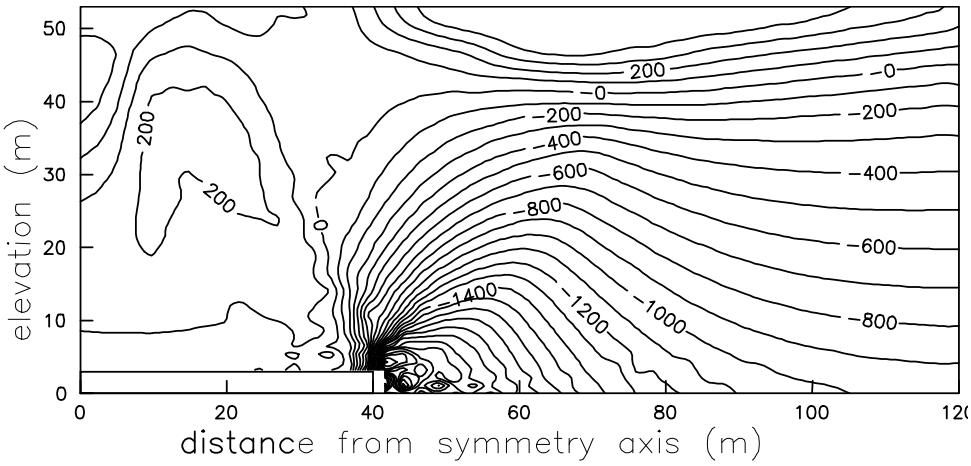

Fig. 18 - Major principal stress contours with K_o = 2.0 and w/h = 1.6

5. RE-ANALYSIS OF SINGARENI COAL MINE SUBSIDENCE

With the experience gained from the above parametric studies, it could be said that the panel width (w) should be less than or equal to 1.2 times the overburden depth to minimise the surface subsidence. The Singareni coal mines case was re-analysed with smaller panel width of 120 m (i.e. with

w/h=1.2) to examine its influence on the subsidence while keeping all other parameters the same. The surface subsidence has decreased drastically as shown in Fig. 19. This clearly shows that the panel width has significant influence on the surface subsidence, especially in this case with low K_o value.

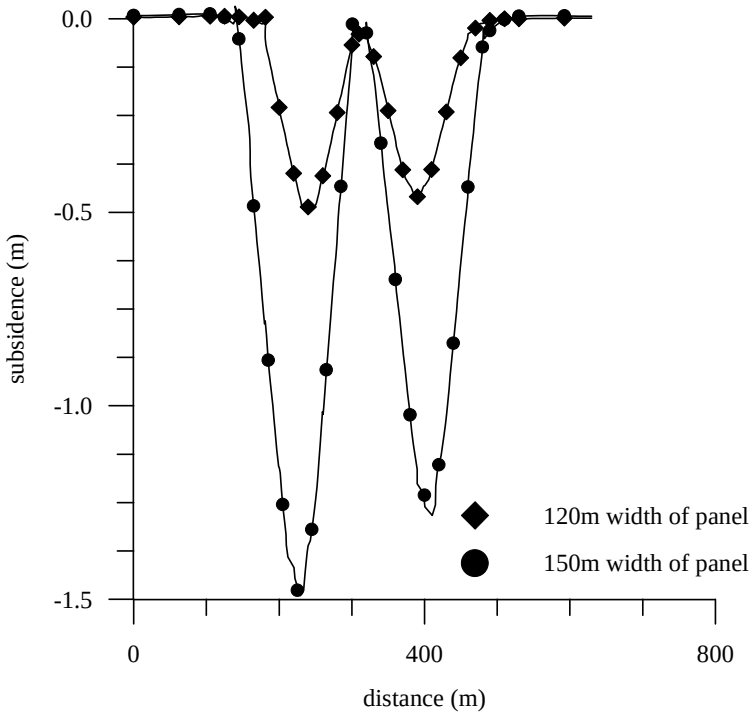

Fig. 19 - Influence of panel width on surface subsidence at Singareni coal mines

6. CONCLUSIONS

The subsidence, which is produced as a result of underground mining operations, has many serious undesirable effects and hence its understanding is of prime importance, especially for giving reliable predictions of its occurrence. The advent of computers and their usage in the mining research has paved the way for subsidence prediction techniques. Hence in this context, a 2-D numerical finite element model was developed for predicting subsidence and the effect of various parameters on the surface subsidence was studied in detail in the present work. Based on the results obtained from this investigation, the following conclusions are drawn.

1. Finite element techniques can be employed to accurately predict the surface subsidence due to mining activities. Using these methods, it is possible to determine the optimum panel and pillar widths that give the maximum coal extraction while mining induced subsidence is kept to a minimum.
2. The discontinuous nature of the rock is responsible to a large extent in effecting the surface subsidence. The behaviour of the rock joints can be

simulated using the 6-node joint elements and the data from direct shear tests on these interfaces.

3. The critical width of panel beyond which the surface subsidence increases tremendously can be said to be equal to 1.2 times the overburden depth.
4. The width of the pillar between the panels also influences the surface subsidence to a large extent.
5. The in situ earth pressures influence the subsidence only when the width of excavation is near to the critical value. At higher K_o values, critical *w/h* value is higher than that at lower K_o values.
6. Apart from the w/h ratio, the subsidence is also dependent on the depth of overburden and the thickness of the excavated zone.

References

Choi D.S., and Dahl, H.D (1981) Measurement and prediction of mine Subsidence over room and pillar in three dimensions, Proc. of the Workshop on Surface Subsidence Due to Underground Mining, West Virginia University, Morgantown, USA 34-47.

Kohli, K.K. (1984) Prediction of surface subsidence profile due to underground mining in the Appalachian coalfield, *PhD* Dissertation, West Virginia University, Morgantown, WV, USA.

Naik, S. and Rao, V.R.R. (1999) "Subsidence Predictions Using Discontinuum Models for Longwall Excavations at Singareni Coal Fields", *Platinum Jubilee Symposium on Productivity Improvement in Mining Industry*, Varanasi, January, 360-372.

Rajagopal, K. (1998) User's Manual for the Finite Element Program GEOFEM, Department of Civil Engineering, Indian Institute of Technology Madras, Chennai.

Ramakanth, P.L.S. (2000) Finite Element Analysis of Subsidence in Long Wall Coal Mines, Thesis submitted for the award of the Master of Science degree by research, Indian Institute of Technology Madras, Chennai.

Singh, M.M. (1978) Experience with Subsidence Due to Mining, Proc. Int. Conf. on Evaluation and Prediction of Subsidence, ASCE, New York, 92-112.

Siriwardane, H.J. (1985) A numerical procedure for prediction of subsidence caused by longwall mining, Proc. 5th Int. Conf. on Num. Meth. In Geomechanics, Boston, A.A. Balkema, 1595-1602.

Su, W.H. (1992) Finite Element Modelling of subsidence induced by underground coal mining. 3rd Subsidence Workshop Due to Underground Mining, June, Morgantown, USA, 32-46.